

## Supplementary Figure Legends

Supplementary Figure 1: Representative collision induced dissociation (CID) spectra from each class of lipid observed in the MALDI imaging experiments including (A)  $[M+Na]^+$  of TAG(52:2) ( $m/z$  881.8), (B)  $[M+Na]^+$  of PC(34:1) ( $m/z$  782.6) (C)  $[M+H-H_2O]^+$  of Cer(d18:1/18:0) ( $m/z$  548.5), (D)  $[M-H]^-$  of PI(18:0/20:4) ( $m/z$  885.6), (E)  $[M-H]^-$  of PE(P-18:1/18:1) ( $m/z$  726.7), and (F)  $[M-H]^-$  of PS(18:0/22:6) ( $m/z$  834.6).

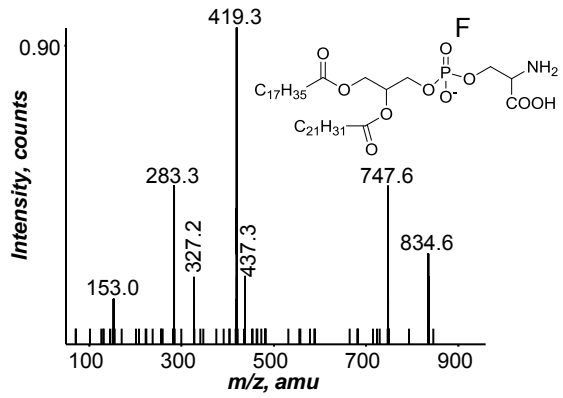
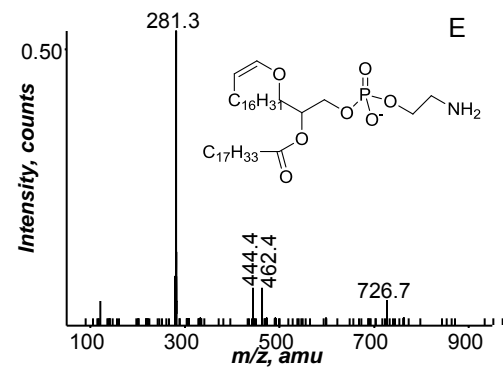
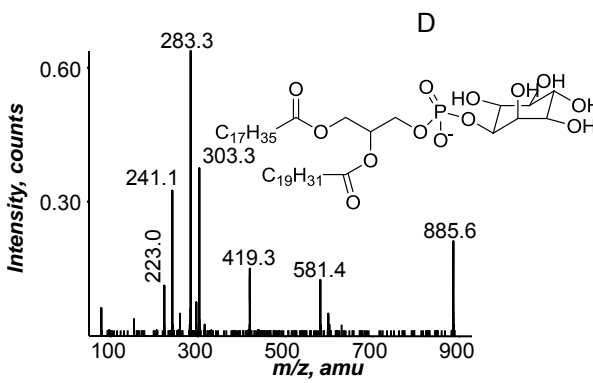
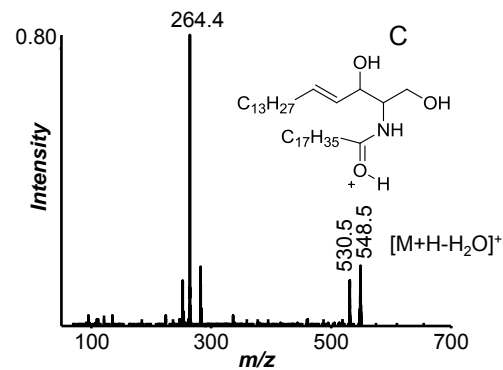
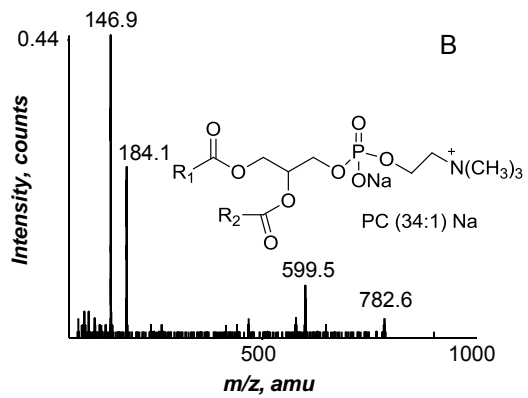
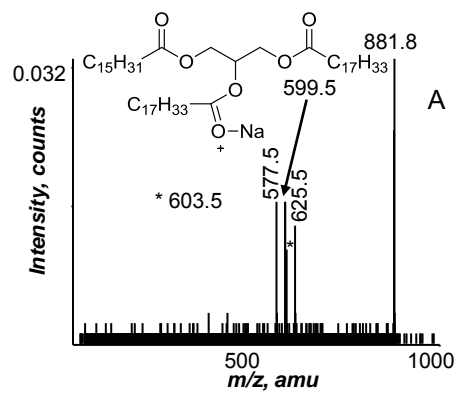
Supplementary Figure 2: Extracted positive ion MALDI images of the (A)  $[M+Na]^+$  of PC(38:4) at  $m/z$  832.6, (B)  $[M+Na]^+$  of SM(d18:1/16:1) at  $m/z$  723.6, (C)  $[M+Na]^+$  of PC(32:0) at  $m/z$  756.6, (D)  $[M+H]^+$  of PC(34:1) at  $m/z$  760.6, (E)  $[M+H]^+$  of PC(36:1) at  $m/z$  788.6, (F)  $[M+H]^+$  of PC(40:6) at  $m/z$  834.6, and (G)  $[M+Na]^+$  of PC(38:6) at  $m/z$  828.6.

Supplementary Figure 3: (A) Negative ion MALDI mass spectrum of PC(16:0/18:1) standard with DHAP matrix. (B) Negative ion CID of  $m/z$  910.7, which is  $[M-H]^-$  of the DHAP adduct of PC(16:0/18:1).

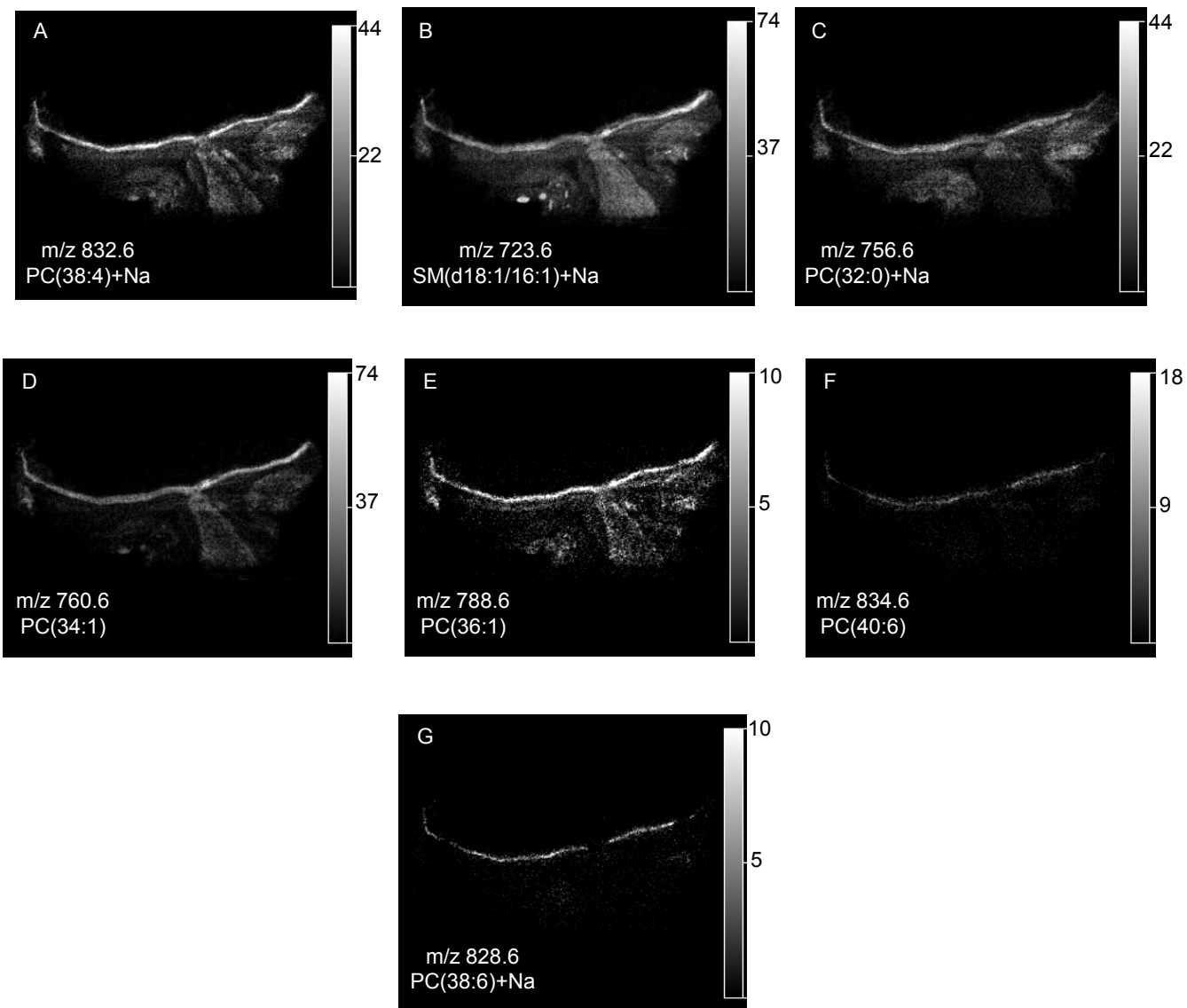
Supplementary Figure 4: Extracted negative ion MALDI images of the (A)  $[M+H]^-$  of PS(18:0/18:1) at  $m/z$  788.5, (B)  $[M+H]^-$  of PS(18:0/20:4) at  $m/z$  810.5, (C)  $[M+H]^-$  of PE(P-16:0/18:1) at  $m/z$  700.5, (D)  $[M+H]^-$  of PE(P-18:0/18:1) at  $m/z$  728.5, (E)  $[M+H]^-$  of ST(18:0/h24:1) at  $m/z$  904.7, (F)  $[M+H]^-$  of ST(18:0/24:1) at  $m/z$  888.7, (G)  $[M+H]^-$  of PE(P-18:0/20:4) at  $m/z$  750.5, (H)  $[M+H]^-$  of PE(18:0/20:4) at  $m/z$  766.5, and (I)  $[M+H]^-$  of PE(16:0/22:6) at  $m/z$  762.5.

Supplementary Figure 5: Extracted positive ion MALDI images of ions originating from the embedding compound at (A)  $m/z$  909.3, (B)  $m/z$  951.3, (C)  $m/z$  1009.3, and (D)  $m/z$  1067.3 and

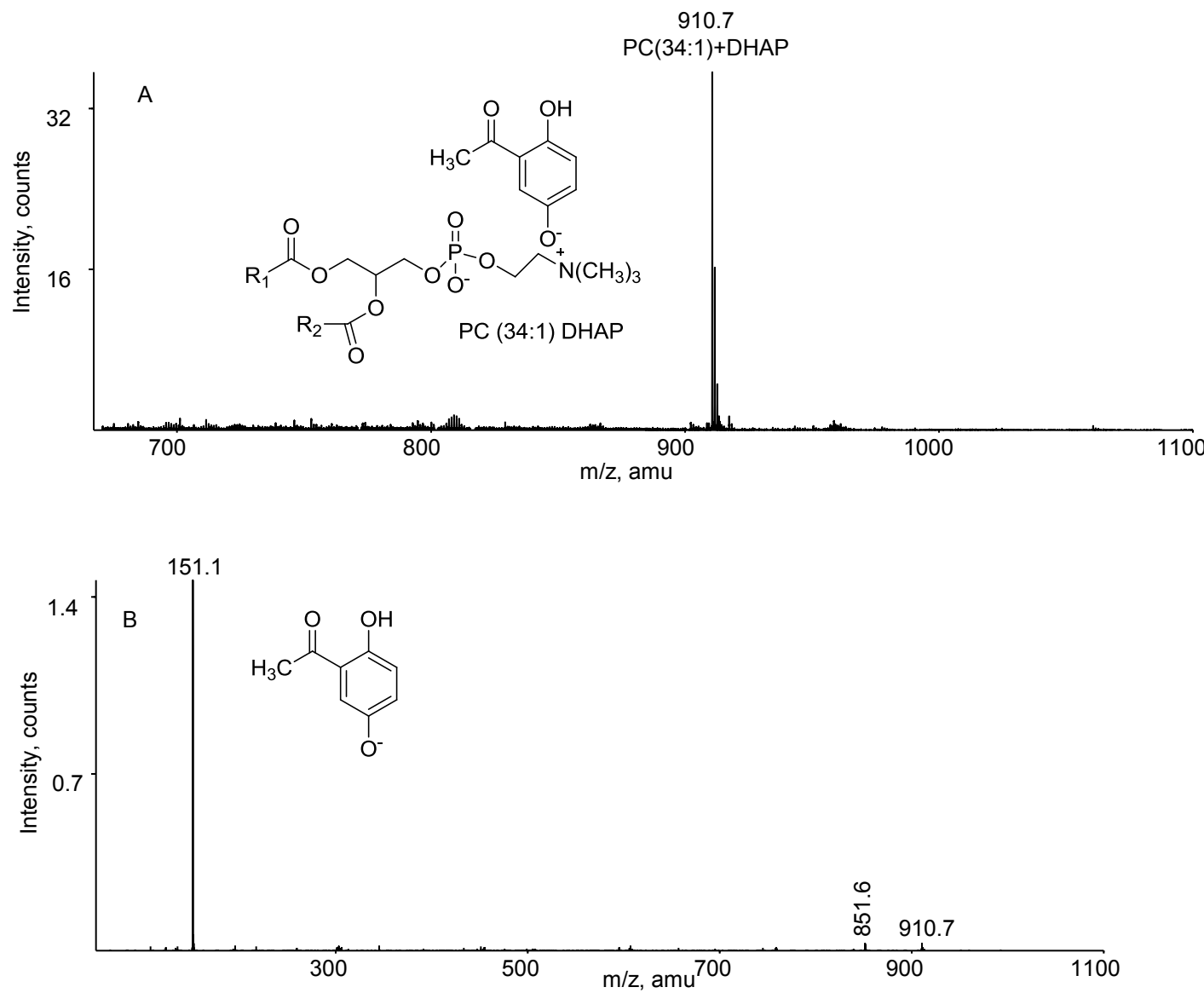
from the  $[M+Na]^+$  of (E) PC(54:12) at m/z 1040.7, (F) PC(54:11) at m/z 1042.7, and (G) PC(54:10) at m/z 1044.7.



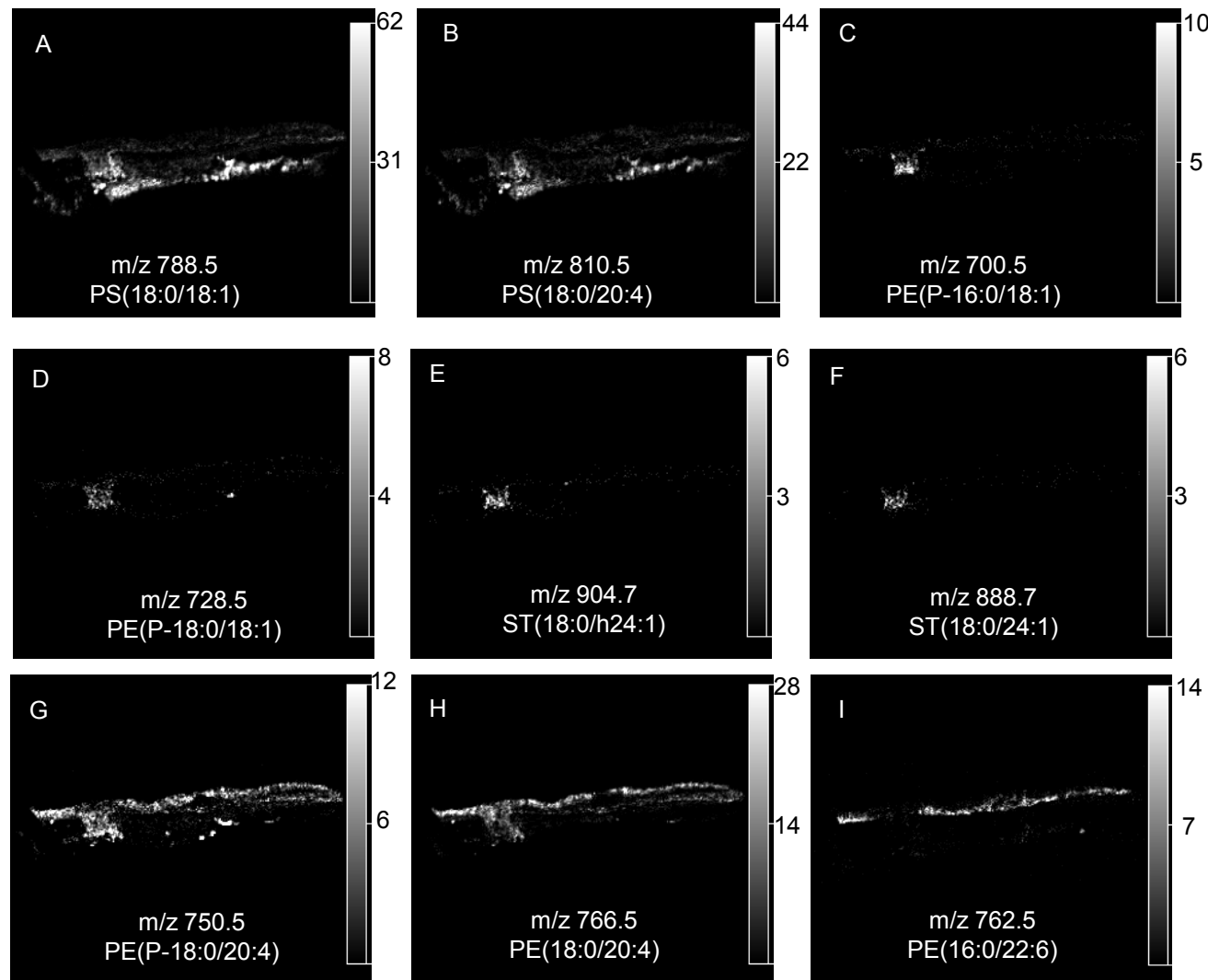
Supplementary  
Figure 1



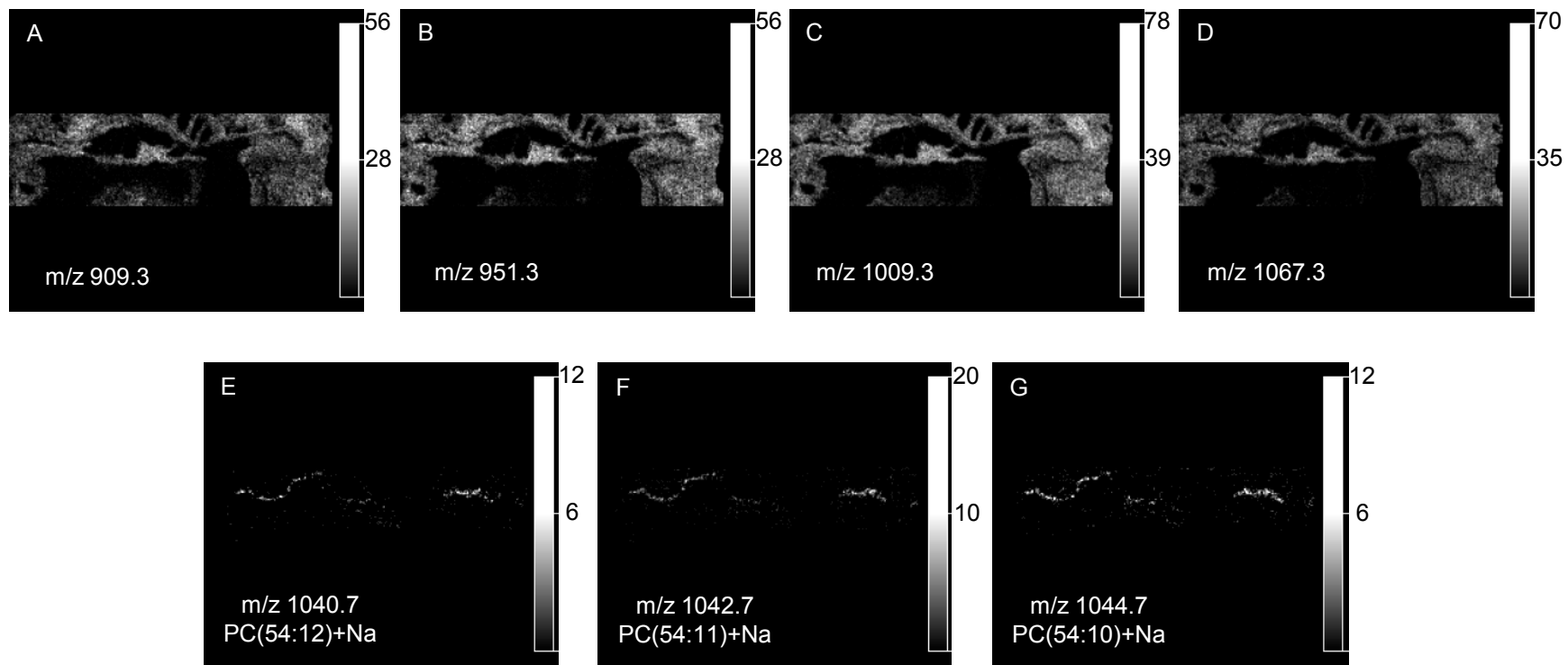
Supplementary  
Figure 2



Supplementary  
Figure 3



Supplementary  
Figure 4



Supplementary  
Figure 5